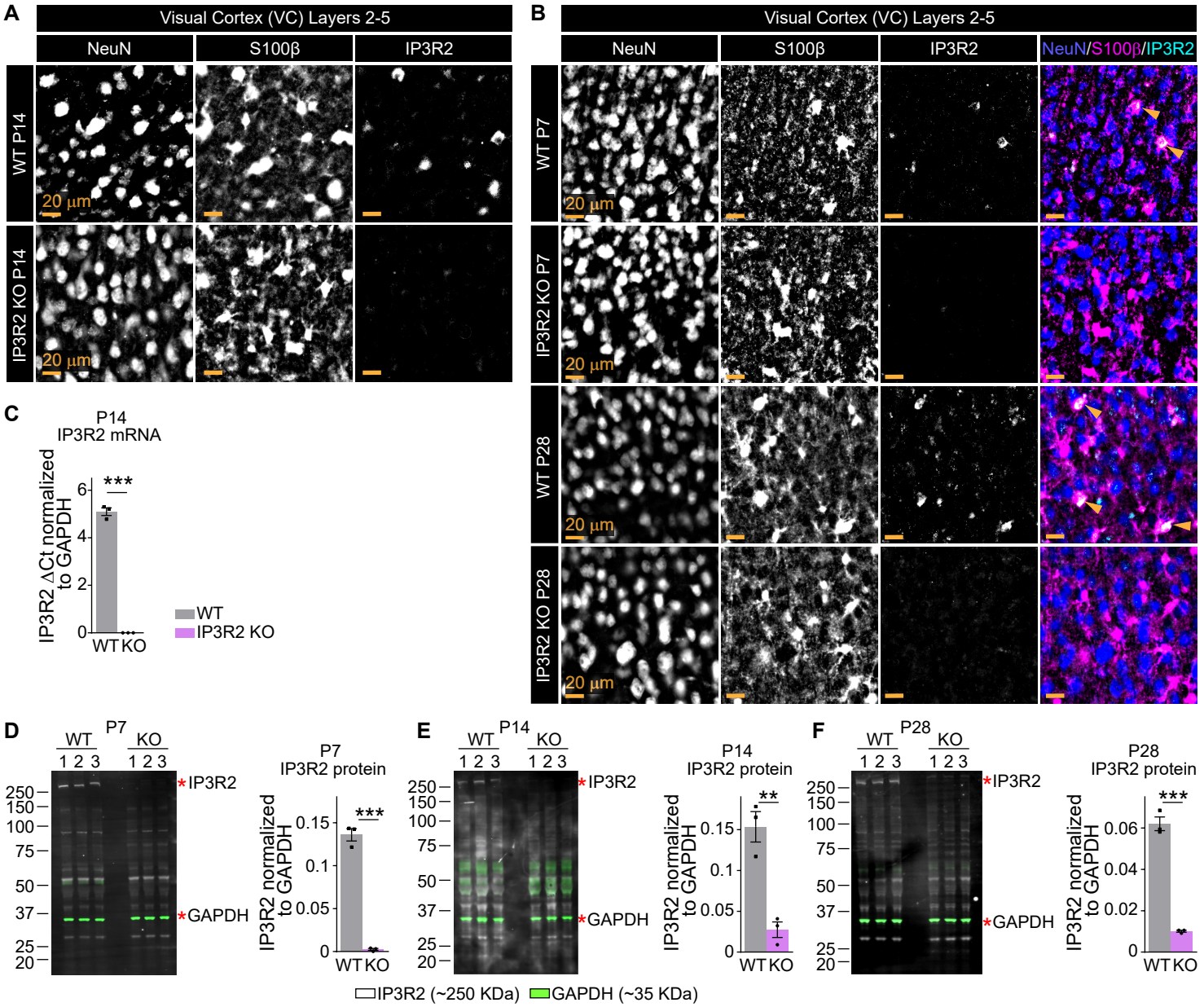
A
Visual Cortex (VC) Layers 2-5
NeuN
S100β
IP3R2
WT P14
IP3R2 KO P14
20 μm
B
Visual Cortex (VC) Layers 2-5
NeuN
S100β
IP3R2
NeuN/S100β/IP3R2
WT P7
IP3R2 KO P7
WT P28
IP3R2 KO P28
20 μm
C
P14
IP3R2 mRNA
IP3R2 ΔCt normalized to GAPDH
***
WT
IP3R2 KO
D
P7
WT
KO
1 2 3
*IP3R2
*GAPDH
P7
IP3R2 protein
IP3R2 normalized to GAPDH
***
E
P14
F
P28
**
IP3R2 (~250 KDa)
GAPDH (~35 KDa)
G
Visual Cortex (VC) Layer 1; Wild type
VGLUT2
PSD95
VGLUT2 / PSD95
WT P7
WT P14
WT P28
5 μm
H
Visual Cortex (VC) Layer 1; IP3R2 KO
IP3R2 KO P7
IP3R2 KO P14
IP3R2 KO P28

Figure S1

Figure S1. Glutamatergic synapse development is perturbed in IP3R2 KO mice VC, related to Figure 1. See also Table S1. **A.** Example single channel grayscale images of P14 VC in WT and KO mice as labeled showing Neun, S100β, and IP3R2 signal (merged image is shown in Fig. 1B). **B.** Example images of Neun, S100β and IP3R2 in WT and KO VC at P7 and P28 as labeled. Single channel grayscale images are on the left, merged images on the right. **C.** Quantification of qPCR represented as change in IP3R2 Ct (ΔCT) relative to GAPDH. IP3R2 mRNA was not detectable in IP3R2 KO mice. **D-F.** Uncropped Western Blot images showing IP3R2 signal (white; imaged at 700 channel; see Methods) and GAPDH signal (green imaged at 800 channel) for each age and genotype as labeled. Numbers above each lane indicate individual mouse samples. For each blot, quantification is shown on the right, represented as IP3R2 signal normalized to GAPDH loading control for each age and genotype as labeled. IP3R2 signal is strongly reduced in IP3R2 KO mice at all developmental stages. **G-H.** Example images of the presynaptic VGLUT2, postsynaptic PSD95 and merged (synapses) in each age and genotype as labeled. Single channel grayscale images on the left, merged images on the right. Graphs show mean ± s.e.m. Individual mouse data points are shown as circles. Number of mice/group (N) N=3 in A-F; N=5 in G-H. Scale bar = 20 μm in A-B; 5 μm in G-H. Arrowheads mark representative IP3R2 signal colocalized with astrocyte marker S100β in B, and colocalized puncta in G-H. **P<0.01; ***P<0.001 comparing WT and KO groups by t-test. ns denotes non-significant (P>0.05) results.

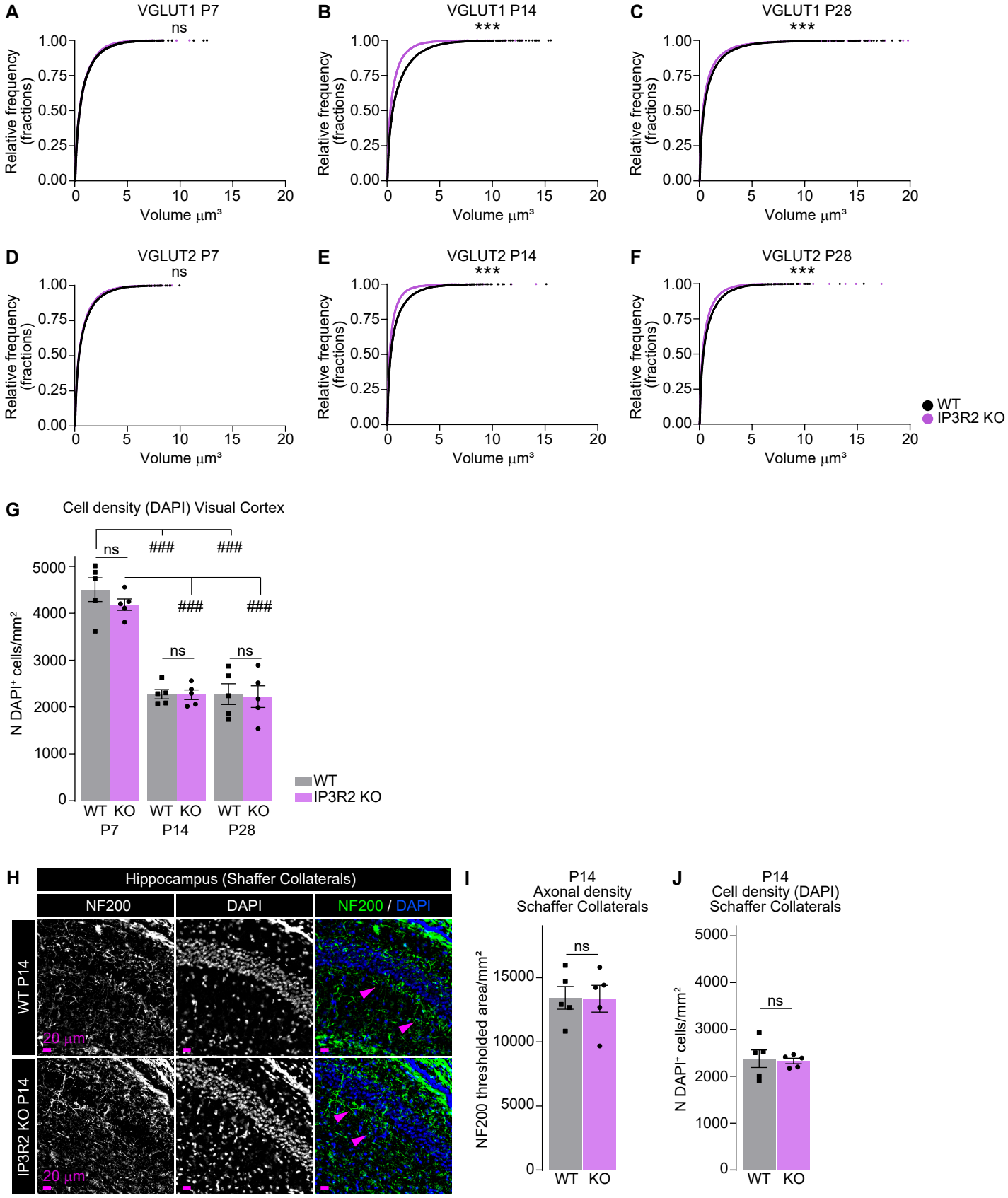
A
VGLUT1 P7
ns
B
VGLUT1 P14
***
C
VGLUT1 P28
***
D
VGLUT2 P7
ns
E
VGLUT2 P14
***
F
VGLUT2 P28
***
Relative frequency (fractions)
Volume µm³
WT
IP3R2 KO
G
Cell density (DAPI) Visual Cortex
N DAPI⁺ cells/mm²
ns
###
WT KO
P7
P14
P28
H
Hippocampus (Shaffer Collaterals)
NF200
DAPI
NF200 / DAPI
WT P14
IP3R2 KO P14
20 µm
I
P14
Axonal density
Schaffer Collaterals
NF200 thresholded area/mm²
J
P14
Cell density (DAPI)
Schaffer Collaterals

Figure S2

Figure S2. VGLUT volumes are reduced in IP3R2 KO mice with no change in cell numbers, related to Figures1-2. See also Table S1. **A-F.** Cumulative distributions of volumes from 3D Imaris rendered images (see Fig. 1, Fig. S1) for VGLUT1 (**A-C**) and VGLUT2 (**D-F**) per age and genotype as labeled. Higher fraction of smaller volumes (<5 μm^3) is observed in IP3R2 KO mice at P14 and P28, but not P7. ***P<0.001 by Kolmogorov-Smirnov test comparing WT and KO within each age. ns denotes non-significant results (>0.05). **G.** Quantification of Fig. 2A-B showing cell density (represented by number of DAPI positive ($^+$) cells normalized to total area) is decreased across development from P7 to P28 similarly in WT and KO groups, with no difference between genotypes at any age tested. **H.** Hippocampal Schaffer collateral axon density is similar at P14 in WT and IP3R2 KO mice. Representative images of hippocampus in WT (left) and IP3R2 KO (right) labeled for NF200 and DAPI. Arrows indicate representative Schaffer collateral axons. **I-J.** Quantification of H showing NF200 (**I**) and DAPI (**J**) cell density. Graphs show mean ± s.e.m. in G, I, J. Individual mouse data points are shown as circles and squares. Number of mice/ group (N) N=5. $^{###}$P<0.001 by one-way ANOVA with post-hoc Tukey's test comparing cell density between age groups within each genotype. ns denotes non-significant (P>0.05) results comparing WT and KO groups by one-way ANOVA in G, and t-test in I-J.

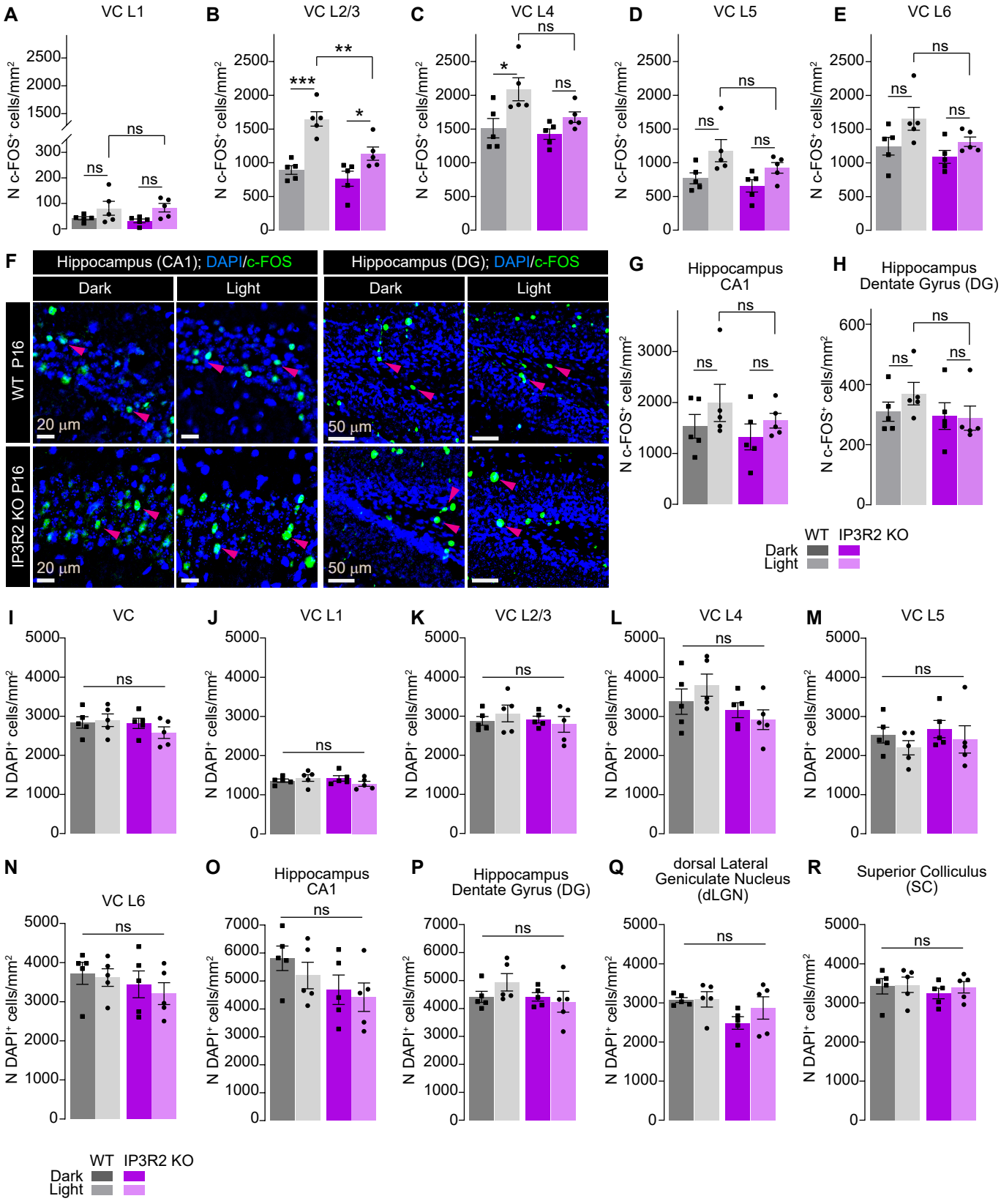
A
VC L1
B
VC L2/3
C
VC L4
D
VC L5
E
VC L6
N c-FOS⁺ cells/mm²
ns
*
**
***
F
Hippocampus (CA1); DAPI/c-FOS
Hippocampus (DG); DAPI/c-FOS
Dark
Light
WT P16
IP3R2 KO P16
20 µm
50 µm
G
Hippocampus CA1
H
Hippocampus Dentate Gyrus (DG)
WT
IP3R2 KO
I
VC
J
VC L1
K
VC L2/3
L
VC L4
M
VC L5
N DAPI⁺ cells/mm²
N
VC L6
O
Hippocampus CA1
P
Hippocampus Dentate Gyrus (DG)
Q
dorsal Lateral Geniculate Nucleus (dLGN)
R
Superior Colliculus (SC)

Figure S4

Figure S4. Light-evoked c-FOS expression is blunted in IP3R2 KO mice visual circuit, related to Figure 4. See also Table S1. **A-E.** Quantification of Fig.4 C-D separated by cortical layers represented as c-FOS positive cell numbers per area (c-FOS cell density). Light exposure induces a significant increase in c-FOS positive cell density in the WT in layers 2/3, and 4, and significant increase in L2/3 in the KO group. Light-evoked c-FOS density is lower in the KO layer 2/3 than WT. **F-H.** Light exposure does not induce increased c-FOS expression in the hippocampus. Example images of c-FOS (green) and DAPI to mark cell nuclei (blue) in the CA1 and DG regions of the hippocampus in both genotypes as labeled (**F**), as well as quantification for CA1 (**G**) and dentate gyrus (DG) (**H**) are shown. No difference is observed between light and dark conditions or the genotypes in either sub-region. **I-R.** Quantification of DAPI positive cells shows no difference between genotypes or light conditions in any of the analyzed brain regions. Graphs show mean ± s.e.m. Individual mouse data points are shown as circles and squares. Number of mice/ group (N) N=5, KO DG N=4. Scale bar CA1 = 20 μm, DG = 50 μm. Arrowheads mark representative c-FOS positive ($^{+}$) cells. *P≤0.05; **P<0.01; ***P<0.001 by one-way ANOVA with post-hoc Šidák's test. ns denotes non-significant results (P>0.05).

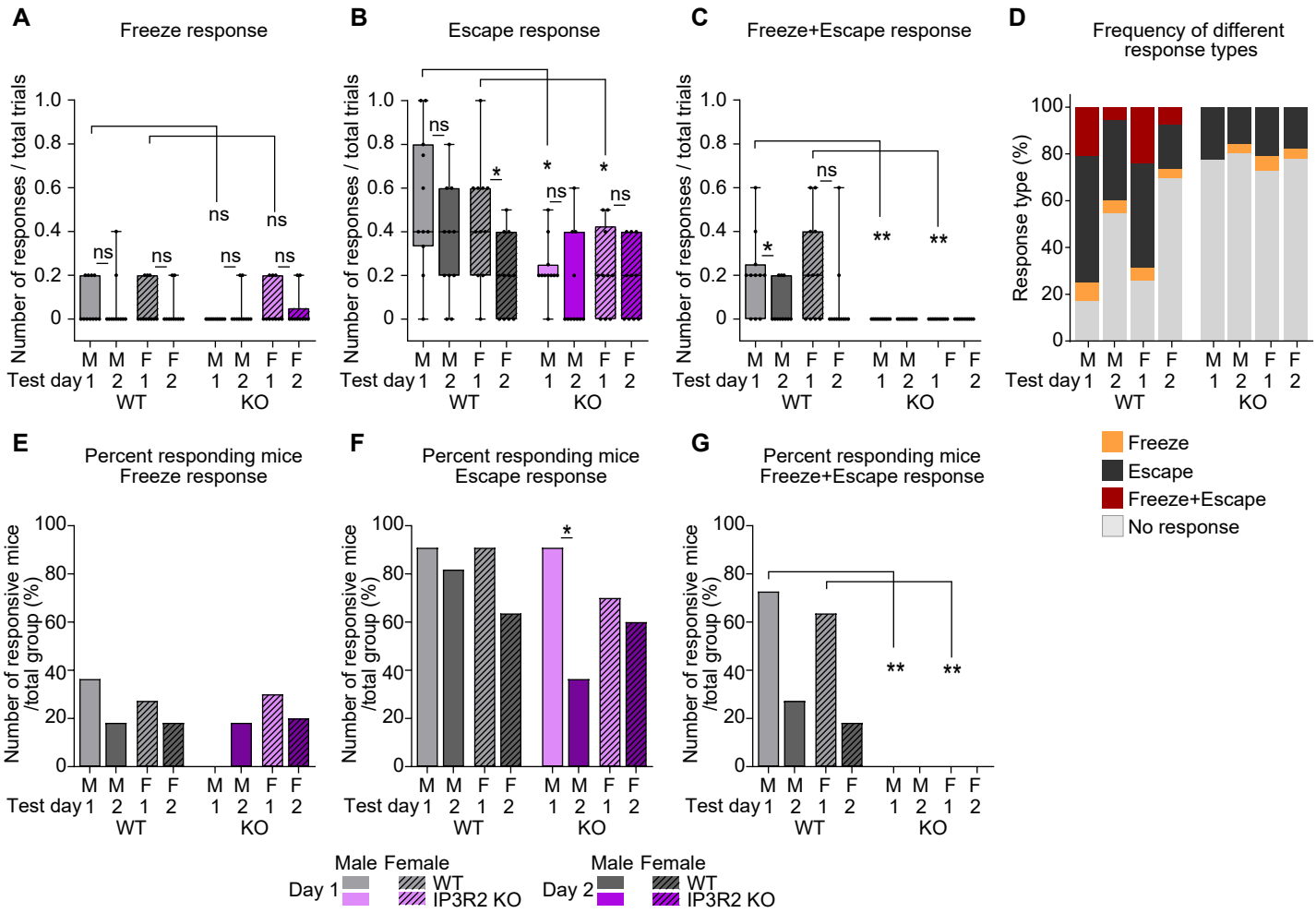
A
Freeze response
B
Escape response
C
Freeze+Escape response
D
Frequency of different response types
Number of responses / total trials
Response type (%)
Test day
WT
KO
Freeze
Escape
Freeze+Escape
No response
E
Percent responding mice
Freeze response
F
Percent responding mice
Escape response
G
Percent responding mice
Freeze+Escape response
Number of responsive mice /total group (%)
Male Female
Day 1
Day 2
WT
IP3R2 KO

Figure S5

Figure S5. Visually evoked defensive behavior is disrupted in IP3R2 KO mice, related to Figure 5. See also Table S1. **A-C.** Average defensive responses separately quantified by response type as labeled (“Freeze”, “Escape”, and “Freeze+Escape”) across genotypes, sexes, and experimental days. “Escape” responses are significantly reduced, and “Freeze+Escape” responses are abrogated in KO mice of both sexes. Freeze responses are not different between genotypes. Graphs show box with range, line is median. Individual mouse data points are shown as circles. **D.** Fractions of each of the defensive response types (“Freeze” – orange; “Escape” – black; “Freeze+Escape” – maroon; “No response” – gray) out of total responses shown as percentage for each age and sex as labeled. **E-G.** Number of responders represented as percentage of mice responding to at least one trial per day out of total group number for each of the response types as labeled. All groups exhibited a similar percentage of responders, except for the “Freeze+Escape” response, which was entirely absent in KO mice. Number of mice (N) N=8-10/ sex/genotype. *P≤0.05; **P<0.01; ***P<0.001 by Mann-Whitney test. ns denotes non-significant results (P>0.05).

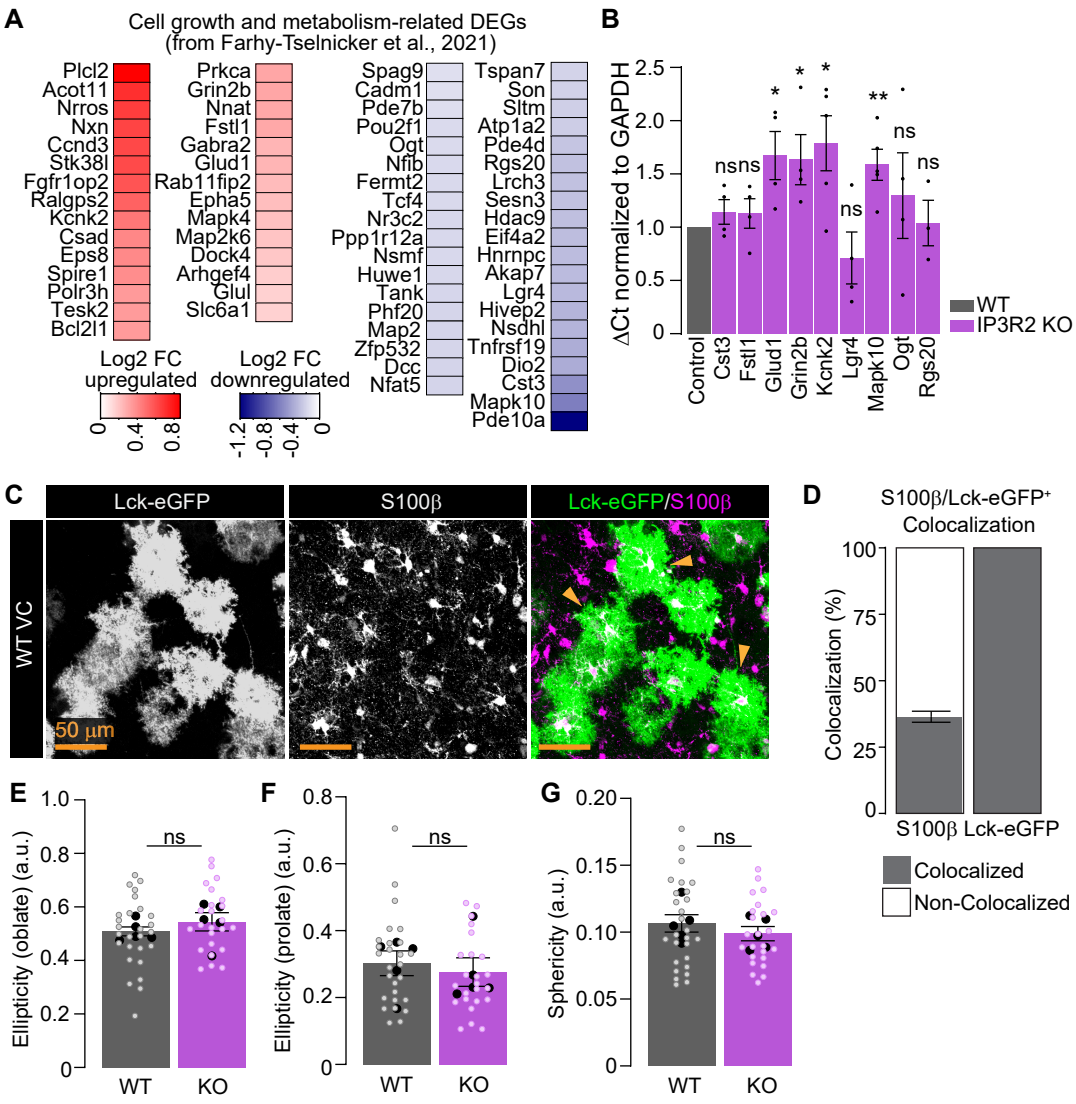
A
Cell growth and metabolism-related DEGs
(from Farhy-Tselnicker et al., 2021)
Plcl2
Acot11
Nrros
Nxn
Ccnd3
Stk38l
Fgfr1op2
Ralgps2
Kcnk2
Csad
Eps8
Spire1
Polr3h
Tesk2
Bcl2l1
Prkca
Grin2b
Nnat
Fstl1
Gabra2
Glud1
Rab11fip2
Epha5
Mapk4
Map2k6
Dock4
Arhgef4
Glul
Slc6a1
Spag9
Cadm1
Pde7b
Pou2f1
Ogt
Nfib
Fermt2
Tcf4
Nr3c2
Ppp1r12a
Nsmf
Huwe1
Tank
Phf20
Map2
Zfp532
Dcc
Nfat5
Tspan7
Son
Sltm
Atp1a2
Pde4d
Rgs20
Lrch3
Sesn3
Hdac9
Eif4a2
Hnrnpc
Akap7
Lgr4
Hivep2
Nsdhl
Tnfrsf19
Dio2
Cst3
Mapk10
Pde10a
Log2 FC upregulated
0
0.4
0.8
Log2 FC downregulated
-1.2
-0.8
-0.4
0
B
ΔCt normalized to GAPDH
2.5
2.0
1.5
1.0
0.5
0
ns
ns
*
*
*
ns
**
ns
ns
Control
Cst3
Fstl1
Glud1
Grin2b
Kcnk2
Lgr4
Mapk10
Ogt
Rgs20
WT
IP3R2 KO
C
Lck-eGFP
S100β
Lck-eGFP/S100β
WT VC
50 μm
D
S100β/Lck-eGFP+
Colocalization
Colocalization (%)
100
75
50
25
0
S100β Lck-eGFP
Colocalized
Non-Colocalized
E
Ellipticity (oblate) (a.u.)
1.0
0.8
0.6
0.4
0.2
0
ns
WT
KO
F
Ellipticity (prolate) (a.u.)
0.8
0.6
0.4
0.2
0
ns
WT
KO
G
Sphericity (a.u.)
0.20
0.15
0.10
0.05
0
ns
WT
KO

Figure S6

Figure S6. Reduced morphology in IP3R2 KO astrocytes, related to Figure 6. See also Table S1. **A.** Heatmap showing Log2 fold change for cell growth and metabolism-related differentially expressed genes (DEGs; obtained from published single nucleus RNA sequencing dataset, Farhy-Tselnicker et al., 2021[4]) in IP3R2 KO mice relative to WT. **B.** Quantification of qPCR represented as change in IP3R2 KO Ct (ΔCT) relative to GAPDH normalized to WT ΔCT. Number of mice/group (N) N=3-5 per gene, each reaction run in triplicates. *P≤0.05; **P<0.01; ns denotes non-significant results (P>0.05) by t-test. **C-D.** Validation of AAV expression showing specificity and sparsity of Lck-eGFP labeling in VC astrocytes. Example images showing Lck-eGFP (green) and astrocyte specific marker S100β (magenta) (**C**) and quantification (**D**). Plot shows percentage of double labeled cells out of total astrocytes (S100β positive) or Lck-eGFP positive showing full overlap of Lck-eGFP expressing cells with S100β within each image. **E-G.** Astrocytic shape characteristics including ellipticity and sphericity are unaltered by IP3R2 KO. Graphs show mean ± s.e.m. Black circles are average of signal in each mouse; colored open circles are data for each astrocyte. Number of mice/group (N) N=5, number of astrocytes = 25-27. Scale bar = 50 μm. ns denotes non-significant results (P>0.05) by t-test.